atmosphere

MDPI

Article

Characteristics of Temporal and Spatial Changes in Ozone and $PM_{2.5}$ and Correlation Analysis in Heilongjiang Province

Lichun Xuan [1,†], Lei Li [2,†], Pengjie Wang [2,*], Yanfeng Xing [2], Chengcheng Feng [2,*] and Rui Zhang [2]

1 School of Chemistry and Materials Science, Heilongjiang University, Harbin 150080, China; 2002069@hlju.edu.cn
2 Heilongjiang Ecological Environment Monitoring Center, Harbin 150056, China; hljemcll@126.com (L.L.); hljemcxyf@126.com (Y.X.); geigei_00@163.com (R.Z.)
* Correspondence: wpj_19900915@126.com (P.W.); zoefeng1987@foxmail.com (C.F.)
† These authors contributed equally to this work and should be regarded as co-first authors.

Abstract: The escalating ambient ozone (O_3) pollution in China has garnered significant attention, necessitating an intensified focus on O_3 pollution control and the coordinated management of $PM_{2.5}$ and O_3. This study reviews and analyzes the spatiotemporal characteristics of O_3 and $PM_{2.5}$ concentrations in 13 cities within Heilongjiang Province from 2019 to 2021. The analysis is based on data sourced from the ecological environment monitoring network. In addition to this, correlation analyses were executed to explore the interaction between the two pollutants. The findings reveal a declining trajectory in $PM_{2.5}$ concentration over the past three years, while O_3 concentration has exhibited an upward trend. Temporally, both O_3 and $PM_{2.5}$ concentrations display pronounced seasonal variations, with peaks evident during the spring and summer (May to July), as well as in the winter (January, February, and December). From a spatial standpoint, elevated O_3 concentrations were identified in the southwestern cities of Harbin, Daqing, and Suihua, while the northwestern cities of Daxinganling and Heihe exhibited comparatively lower O_3 concentrations, but the difference was not significant. Conversely, $PM_{2.5}$ concentrations demonstrated substantial variation among the 13 cities (districts). Regarding their correlation, a noteworthy positive correlation between the two pollutants was observed in April and May, contrasted by a negative correlation in November and December. Weather categories such as excellent, good, lightly polluted, moderately polluted, and other weather showed a lower correlation, whereas heavily polluted and severely polluted categories demonstrated a stronger correlation. Furthermore, the correlation with severe pollution is greater than that with heavily polluted, further indicating that heavier air pollution is more conducive to the coexistence of O_3 and $PM_{2.5}$ to form composite pollution. On a provincial scale, the correlation between the two pollutants is progressively increasing annually. This signifies a closely intertwined and intricate interaction and transformation relationship between O_3 and $PM_{2.5}$, accentuating the urgency for synergistic control measures.

Keywords: Heilongjiang Province; ozone; $PM_{2.5}$; spatial and temporal variations; correlation analysis

Citation: Xuan, L.; Li, L.; Wang, P.; Xing, Y.; Feng, C.; Zhang, R. Characteristics of Temporal and Spatial Changes in Ozone and $PM_{2.5}$ and Correlation Analysis in Heilongjiang Province. *Atmosphere* **2023**, *14*, 1526. https://doi.org/10.3390/atmos14101526

Academic Editors: Nima Afshar-Mohajer and Kumar Vikrant

Received: 24 August 2023
Revised: 23 September 2023
Accepted: 30 September 2023
Published: 2 October 2023

1. Introduction

Ongoing economic development and urbanization have exacerbated atmospheric environmental pollution, which remains a pivotal environmental challenge for China. Currently, China grapples with regional composite pollution, primarily driven by ozone (O_3) and $PM_{2.5}$ [1–3], embodying prevailing atmospheric pollution attributes. This composite pollution significantly impedes a persistent improvement in our air quality, eliciting widespread concern and becoming the nucleus of the present atmospheric pollution control and an important direction of environmental management. Its impact on human health and the ecological environment is unignorable.

O_3, classified as a potent oxidant [4], constitutes a secondary pollutant engendered via the photochemical reaction of volatile organic compounds (VOCs) and nitrogen oxides

(NOx) released from pollution sources under solar irradiation. It is responsible for adverse effects on the human respiratory [5–7], immune [6], and cardiovascular systems [7], as well as the growth and development of flora [8,9]. Conversely, $PM_{2.5}$ particulate constitutes minuscule particulate matter with a diameter not surpassing 2.5 μm, facilitating its entry into the human respiratory tract and subsequently the lungs. This ingress inflicts harm on the respiratory system and cardiovascular system [10–13]. Notably, it can be directly emitted from pollution sources (e.g., road dust, building construction dust, coal combustion dust) [14–16]. Alternatively, it can arise through atmospheric photochemistry, heterogeneous reactions, and other processes, yielding secondary formation (e.g., secondary sulfate, secondary nitrate, and secondary organic matter) [17–20].

Research indicates a multifaceted interaction between O_3 and $PM_{2.5}$. O_3 profoundly influences the chemical mechanisms underlying $PM_{2.5}$ formation [21–24]. Furthermore, near-surface O_3 levels stimulate the production of secondary particulate matter (SPM) by modifying atmospheric oxidative characteristics [25,26]. However, diminished O_3 concentrations do not favor the generation of SPM [27]. Likewise, $PM_{2.5}$ impacts the production and mitigation of O_3. Diminishing $PM_{2.5}$ concentrations were found to be correlated with elevated ozone levels [28], chiefly due to $PM_{2.5}$'s modulation of solar radiation and its influence on atmospheric heterogeneous reaction procedures. A decrease in $PM_{2.5}$ concentration was found to be associated with a surge in ozone concentration [28], primarily attributed to PM's role in influencing the near-surface O_3 concentration through the modulation of solar radiation and alterations to atmospheric heterogeneous reaction processes [29–31].

Situated as a vital hub for food, forest resources, and energy in China, Heilongjiang Province occupies a strategic position as a northern frontier region, endowed with distinctive geographical and climatic attributes that give rise to ambient air pollution challenges. Presently, while the number of national inquiries into O_3 and $PM_{2.5}$ pollution traits and trends continues to rise, the displayed trends and configurations exhibit pronounced divergence across distinct areas. Hence, the deployment of distribution models from other regions cannot be straightforwardly extrapolated to depict the precise circumstances prevailing in Heilongjiang Province. This study comprehensively encompasses all prefecture-level cities within Heilongjiang Province. It scrutinizes the multifaceted changes in O_3 and $PM_{2.5}$ characteristics from 2019 to 2021, assessing the O_3-$PM_{2.5}$ correlation on an expansive scale and from diverse perspectives. The overarching goal is to furnish a scientific foundation for ameliorating the current composite pollution state of air quality in Heilongjiang Province. Moreover, this study strives to supply vital technical backing for orchestrating integrated O_3 and $PM_{2.5}$ management and regulation across cities, encompassing temporal and regional strategies. Additionally, this study extends substantial technical support for harmonized O_3 and $PM_{2.5}$ control endeavors.

2. Sources and Methods

2.1. Data Sources

In this paper, the geographical scope includes Heilongjiang Province, encompassing all cities above the prefecture level. The cities include Harbin, Qiqihar, Mudanjiang, Jiamusi, Daqing, Jixi, Shuangyashan, Yichun, Qitaihe, Hegang, Heihe, Suihua, and Daxinganling. The dataset originates entirely from air pollutant concentration data provided by the Ecological Environment Monitoring Centre of Heilongjiang Province, spanning from 2019 to 2021, and is expressed in micrograms per cubic meter (μg/m^3). The dataset comprises hourly and daily measurements of O_3 and $PM_{2.5}$ concentrations. Additionally, month-to-month and year-to-year concentration data were acquired using rigorous statistical analysis and calculations. Notably, the O_3 concentration represents the daily maximum 8 h sliding average, excluding hourly readings. For the purpose of this study, the seasonal divisions are defined as follows, March to May as spring, June to August as summer, September to November as autumn, and January, February, and December as winter.

2.2. Research Methodology

The data in this paper underwent processing and analysis using Excel, Argis, and Origin software. During the analysis process, linear regression analyses and the correlation coefficient method were used to investigate the relationship between O_3 and $PM_{2.5}$. The assessment of date was conducted based on the guidelines outlined in the Ambient Air Quality Standard (GB 3095-2012), Technical Regulation on Ambient Air Quality Index (AQI) (on trial) (HJ 633-2012), and Technical Specification for Ambient Air Quality Evaluation (on trial) (HJ 663-2013).

The ambient air quality is evaluated using the ambient air quality index (AQI). AQI is divided into six levels, "$0 \leq AQI \leq 50$" is "Excellent", "$50 < AQI \leq 100$" is "Good", "$100 < AQI \leq 150$" is "Lightly polluted", "$150 < AQI \leq 200$" is "Moderately polluted", "$200 < AQI \leq 300$" is "Heavily polluted", and "$AQI > 300$" is "Severely polluted". The maximum value of the individual air quality index (IAQI) for pollutants ($PM_{2.5}$, PM_{10}, SO_2, NO_2, CO, and O_3) is AQI. The IAQI was calculated using the following equations:

$$IAQI_P = \frac{IAQI_{Hi} - IAQI_{Lo}}{BP_{Hi} - BP_{Lo}} \left(C_p - BP_{Lo}\right) + IAQI_{Lo} \quad (1)$$

where $IAQI_P$ is the $IAQI$ of pollutant P. C_p is the concentration value of pollutant P, in $\mu g/m^3$. BP_{Hi} is the high value of pollutant concentration limits similar to C_p in Table 1, in $\mu g/m^3$. BP_{Lo} is the lower value of pollutant concentration limits similar to C_p in Table 1, in $\mu g/m^3$. $IAQI_{Hi}$ is the air quality sub-indices corresponding to BP_{Hi} in Table 1. $IAQI_{Lo}$ is the air quality sub-indices corresponding to BP_{Lo} in Table 1.

Table 1. Individual air quality index (IAQI) and corresponding pollutant concentration limits.

IAQI	O_3 Concentration ($\mu g/m^3$)	$PM_{2.5}$ Concentration ($\mu g/m^3$)
0	0	0
50	100	35
100	160	75
150	215	115
200	265	150
300	800	250

3. Results and Discussion

3.1. Time Variation Characteristics of O_3 and $PM_{2.5}$

3.1.1. Year-by-Year Change Characteristics

We identified the year-by-year situation by analyzing the changes in $PM_{2.5}$ and O_3 pollution days (refers to the days when the daily average IAQI of O_3 and $PM_{2.5}$ was greater than 100, excluding days with excellent and good IAQI) from 2019 to 2021. We calculated the number of days with different types of pollution days in 13 cities each year by adding them up separately. In 2019, Heilongjiang Province witnessed 33 days of O_3 pollution days, out of which 32 days were classified as lightly polluted and one day as moderately polluted. Additionally, there were 244 days of $PM_{2.5}$ pollution days, comprising 140 lightly polluted days, 37 moderately polluted days, 50 heavily polluted days, and 17 severely polluted days. The year 2020 recorded 40 days of O_3 pollution days, with 36 days categorized as lightly polluted, and four days categorized as moderately polluted. Furthermore, there were 292 days of $PM_{2.5}$ pollution days, including 184 lightly polluted days, 49 moderately polluted days, 40 heavily polluted days, and 19 severely polluted days. In 2021, the province observed 52 days of O_3 pollution days, with 48 lightly polluted days and four moderately polluted days. Additionally, there were 188 days of $PM_{2.5}$ pollution days, consisting of 139 lightly polluted days, 24 moderately polluted days, 22 heavily polluted days, and three severely polluted days. Evaluating the number of pollution days and shifts in air quality levels from 2019 to 2021 (Figures 1 and 2), it becomes apparent that O_3 pollution in Heilongjiang Province is deteriorating progressively. While the number of days with $PM_{2.5}$ pollution days displays a declining trend, the fluctuations remain substantial, indicating a lack of consistent and substantial decrease. The persistently high number of pollution days underscores that $PM_{2.5}$ continues to be the primary pollutant adversely impacting ambient air quality.

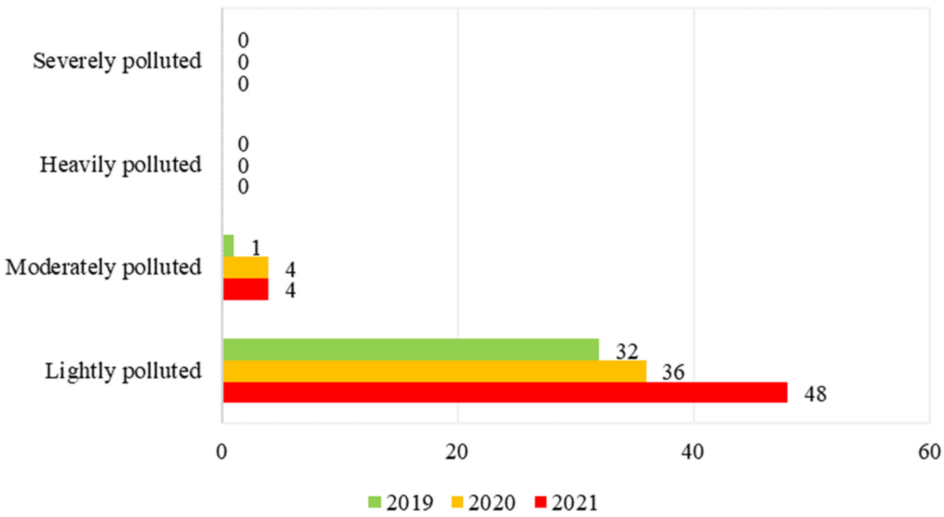

Figure 1. Trends in the number of days of O_3 pollution in different categories in Heilongjiang Province, 2019–2021.

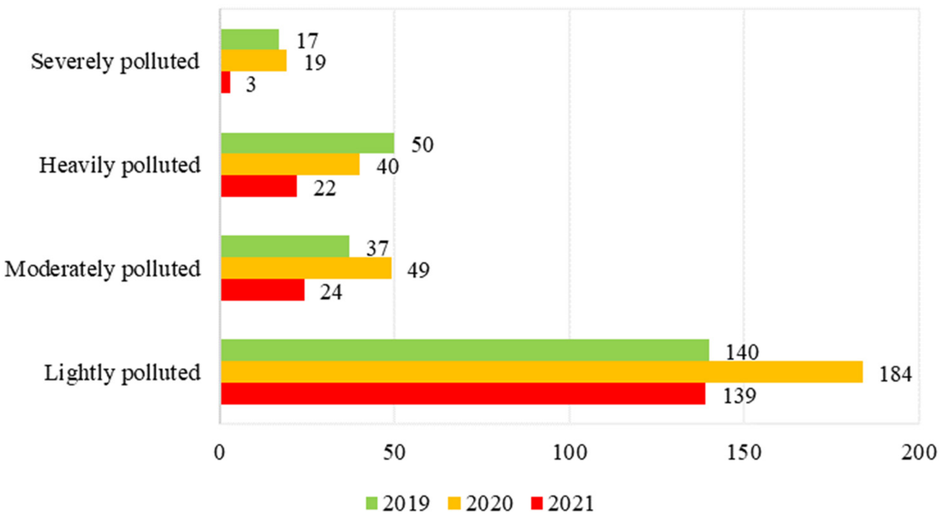

Figure 2. Trends in the number of days of $PM_{2.5}$ pollution in different categories in Heilongjiang Province, 2019–2021.

3.1.2. Month-by-Month Change Characteristics

As depicted in Figure 3, the monthly variation pattern in O_3 in 13 cities across Heilongjiang Province from 2019 to 2021 exhibits a consistent inverted "U" shape. From the perspective of the average monthly concentration in Heilongjiang Province over the three years, O_3 attained its peak in May at 133 $\mu g/m^3$ and its nadir in December at merely 56 $\mu g/m^3$, which is less than half of the peak value. The peak—trough pattern aligns with the nationwide changes. The monthly peaks and troughs in O_3 in Heilongjiang Province mirror the national-scale trends. Specifically, O_3 concentrations were low in January, escalated markedly from February to March, and culminated from April to July, predominantly from May to July. An overall decreasing trend was observed from August to December.

The spring and summer emerge as peak seasons for O_3 pollution in Heilongjiang Province, which is attributed to heightened temperatures, prolonged daylight, and increased light intensity. These factors promoted the photolysis of NOx and enhanced evaporation of VOCs, triggering redox reactions and resulting in accelerated ozone production and elevated O_3 levels [32–34]. It is worth mentioning the significantly higher O_3 concentration in the cities in Heilongjiang Province during 2020 and April 2021 compared with April 2019. These cities were affected by pandemic-induced restrictions on urban traffic and factory operations, coupled with relatively consistent meteorological conditions over the past three years. The surge in O_3 concentration can be attributed to reduced emissions of NO and other ozone-depleting nitrogen oxides (NO_x), which serve as "ozone depleting agents" [35], leading to diminished ozone depletion and consequently higher ozone concentrations. Temporally, strengthening precursor control from April to July—when O_3 pollution is more severe—should be prioritized.

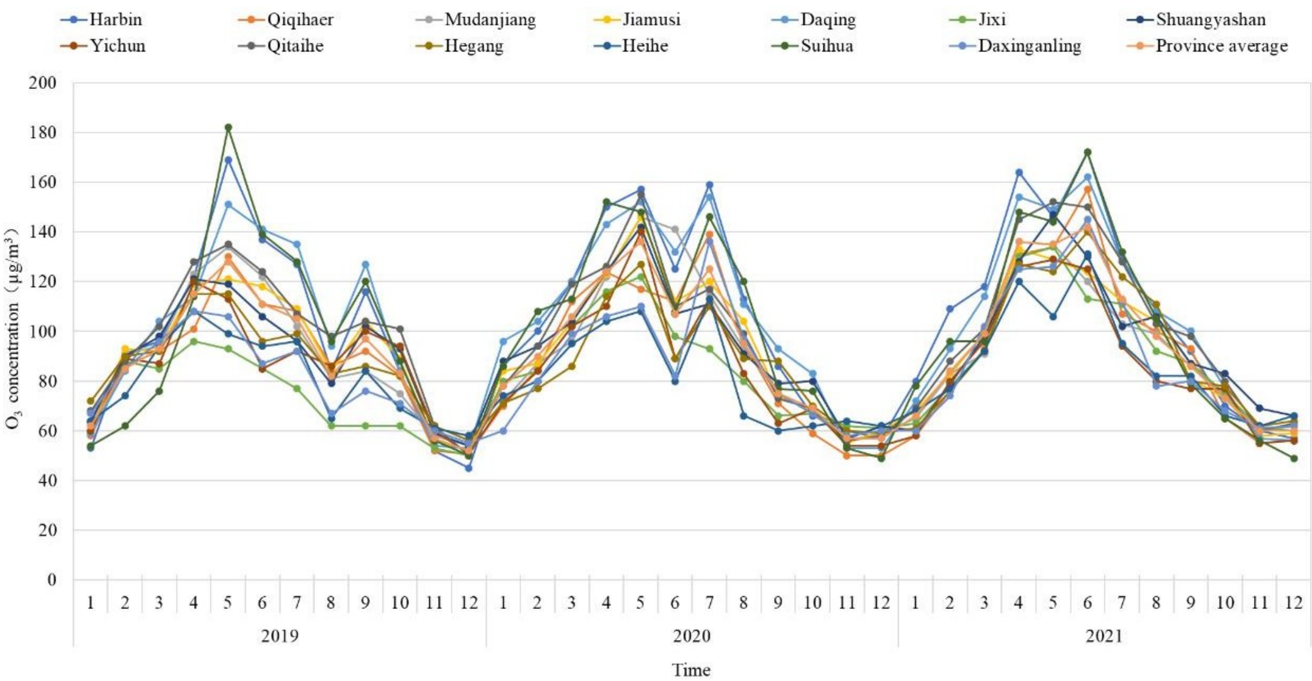

Figure 3. Trend in the monthly average concentration of O_3 in 13 cities in Heilongjiang Province, 2019–2021.

As can be seen in Figure 4, the monthly variation pattern in $PM_{2.5}$ in 13 cities within Heilongjiang Province from 2019 to 2021 stands in contrast to that of O_3, presenting an overall "U" shape. In terms of monthly average concentration, $PM_{2.5}$ reached its peak in January at 56 $\mu g/m^3$, surpassing the Grade 2 standard limit (35 $\mu g/m^3$) defined in the "Ambient Air Quality Standard" (GB 3095-2012). Conversely, the lowest average concentration of $PM_{2.5}$ was observed in August, registering 12 $\mu g/m^3$, which is less than a quarter of the peak value. The concentration trend is highest in January and February, declining each month from March to August, then rebounding sharply from September to December. This disparity indicates higher $PM_{2.5}$ concentrations during the winter compared with the summer, in accordance with nationwide urban trends. However, the variation in $PM_{2.5}$ concentration in Heilongjiang Province is notably more pronounced. This disparity primarily stems from two factors. Firstly, the cold winters in Heilongjiang lead to increased consumption of coal and other energy sources for heating purposes. Some areas still use old household coal-fired boilers, contributing to dispersed air pollutant emissions that prove challenging to effectively mitigate [36]. Secondly, Heilongjiang Province experiences static inverse temperature and other unfavorable meteorological conditions during the winter. Prolonged periods of high humidity coupled with static atmospheric conditions hinder the horizontal and vertical diffusion of atmospheric pollutants, exacerbating the cumulative superposition effect and pollutant concentration [37].

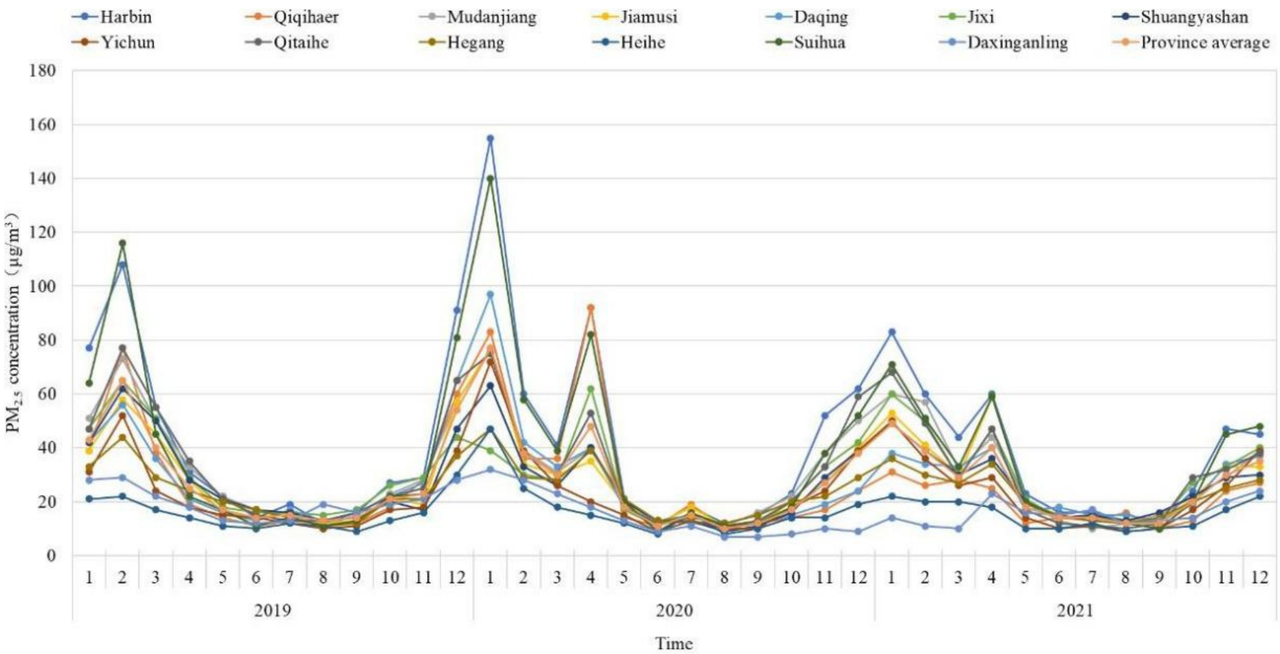

Figure 4. Trend in the monthly average concentration of $PM_{2.5}$ in 13 cities in Heilongjiang Province, 2019–2021.

3.1.3. Hour-by-Hour Change Characteristics

From 2019 to 2021, the hourly changes in the average O_3 concentrations over the three years during different seasons across 13 cities (localities) in Heilongjiang Province are shown in Figure 5. The annual changes from 2019 to 2021 are shown in the Supplementary Materials (Figure S1). The figure demonstrates that the hourly trend in ozone concentrations remains largely consistent over the three-year period, displaying a discernible pattern. O_3 concentrations are lower at night and in the early morning, gradually rising from 5:00 to 8:00 o'clock, peaking at 14:00 o'clock, and then exhibiting a gradual decline with diminishing amplitude until the trend stabilizes. However, variations in O_3 hourly trends among the different seasons are notably distinct. In the spring and summer, O_3 concentrations start to rise from 5:00 or 6:00 o'clock, while in the autumn and winter, this rise is delayed by two hours, commencing at 7:00 or 8:00 o'clock. The swift rise in morning ozone concentration is attributed to the gradual increase in solar radiation and the intensification of O_3 photochemical reactions as the sun ascends. Additionally, the inclination of the Earth's rotation axis contributes to extended sunshine durations to Heilongjiang Province during the spring and summer compared to autumn and winter. This discrepancy manifests as an earlier sunrise and later sunset, leading to earlier O_3 concentration increases in the spring and summer. Conversely, the O_3 concentration starts stabilizing around 18:00 or 19:00 o'clock during the autumn and winter, while this stabilization is notably delayed in the spring and summer, often approaching 0:00 o'clock. The influence of higher nighttime temperatures in the spring and summer accelerates the rate of O_3 decay, resulting in a gradual decrease in ozone concentration. In addition, elevated nighttime temperatures lead to an increase in the height of the atmospheric stabilization layer, accelerating O_3 diffusion and consequently reducing O_3 concentration [38]. From an hourly perspective, if the hourly O_3 concentration exceeds 160 $\mu g/m^3$, swift actions such as organizing inspections for industries, automobile repair businesses, and catering establishments, encouraging nighttime refueling, and promoting eco-friendly commuting between 13:00 and 16:00 o'clock, should be implemented. These measures aim to reduce precursor emissions at the O_3 source and subsequently lower the O_3 concentration.

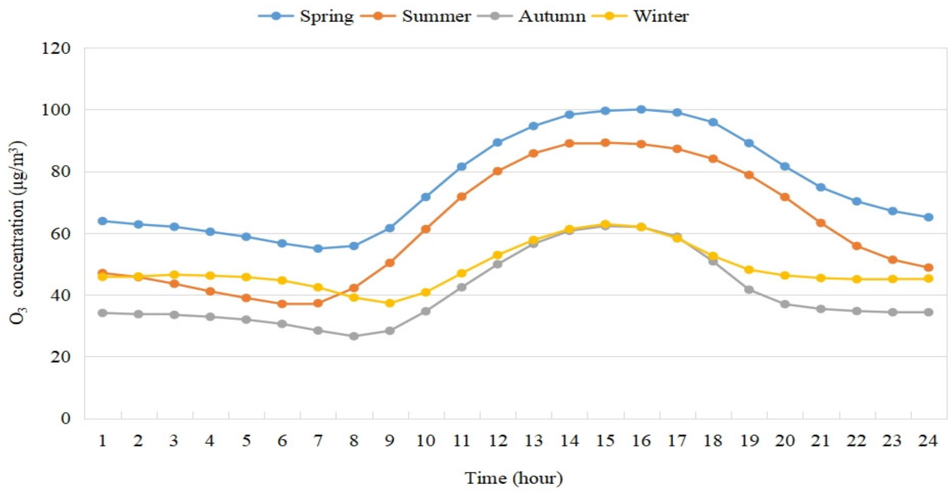

Figure 5. Trends in the monthly mean concentrations of O_3 in 13 cities in Heilongjiang Province.

Figure 6 illustrates the hourly change of average over three years curves of $PM_{2.5}$ during various seasons in 13 cities (districts) within Heilongjiang Province from 2019 to 2021. The annual changes from 2019 to 2021 are shown in the Supplementary Materials (Figure S2). The figure reveals consistent trends in seasonal changes over the past three years. The spring and autumn exhibit an overall shallow "U" shape, while the summer exhibits relatively stable changes. On the other hand, the winter exhibits a distinctive "W" shape, with the most substantial hourly variation among the four seasons. Notably, the $PM_{2.5}$ concentration peaks between 9:00 and 10:00 o'clock and again between 21:00 and 22:00 o'clock during the winter. The morning peak is primarily influenced by anthropogenic factors like transportation and residential heating, while the nocturnal peak is more driven by industrial emissions and heating processes. Moreover, across all four seasons, a $PM_{2.5}$ trough is observed at 15:00 o'clock, followed by a rapid rise culminating around 22:00 o'clock. Beyond the effects of traffic during evening rush hours from 18:00 to 20:00 o'clock, the lower boundary layer height and atmospheric layer stability during the night restrict the vertical dispersion of pollutants, contributing significantly to the nighttime increase in $PM_{2.5}$ concentration.

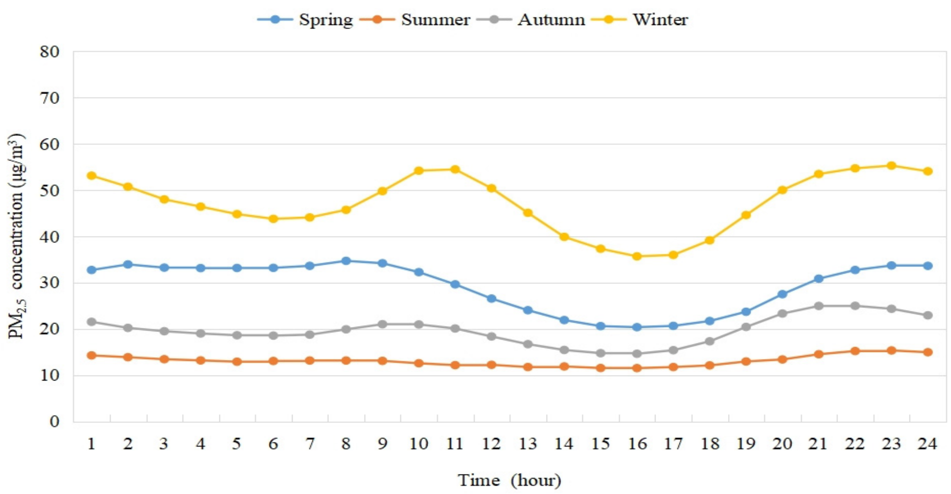

Figure 6. Trends in the monthly mean concentrations of $PM_{2.5}$ in 13 cities in Heilongjiang Province.

3.2. Spatial Variation Characteristics of O_3 and $PM_{2.5}$

The spatial distribution characteristics of the annual mean O_3 concentration within Heilongjiang Province from 2019 to 2021 are shown in Figure 7. The ozone concentration in different regions of Heilongjiang Province exhibits variable patterns. Notably, the southern region (Harbin, QiQihaer, Daqing, and Suihua) experiences evident ozone pollution, while the northeastern region (Jiamusi, Jixi, Shuangyashan, Yichun, Qitaihe, and Hegang) displays relatively higher concentrations. The northwestern region (Heihe, Daxinganling), meanwhile, records the lowest average concentrations. On a local scale, minimal disparity in O_3 concentrations is observed among cities within each region, emphasizing the regionalized nature of O_3 pollution with pronounced transport characteristics [39–43].

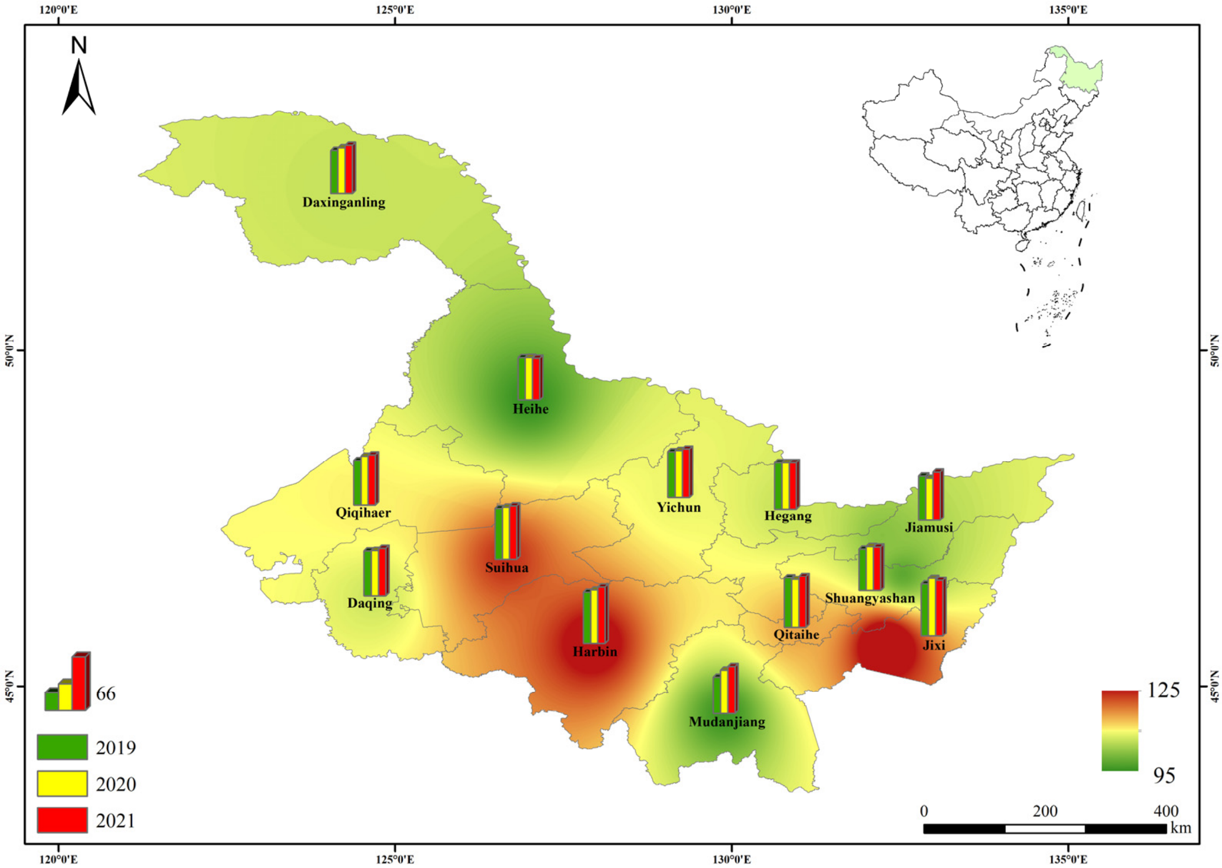

Figure 7. Changes in the annual average concentrations of O_3 in 13 cities in the province, 2019–2021: the background color of the map is the difference between the average values of the three years.

The spatial distribution characteristics of the annual mean $PM_{2.5}$ concentration within Heilongjiang Province from 2019 to 2021 are depicted in Figure 8. In comparison with the regional variability shown by O_3, the variability in $PM_{2.5}$ concentration is more pronounced. While the mean value indicates a sequence of southern region > northeastern region > northwestern region, substantial differences in high and low $PM_{2.5}$ concentrations exist among cities within each region. Notably, the difference in $PM_{2.5}$ concentrations is more significant between Harbin and Qiqihar. Consequently, it is apparent that $PM_{2.5}$ has weak transmission capacity [43–45], with a relatively limited spatial distribution range, especially under static and stable weather conditions, predominantly affected by local regional pollution sources.

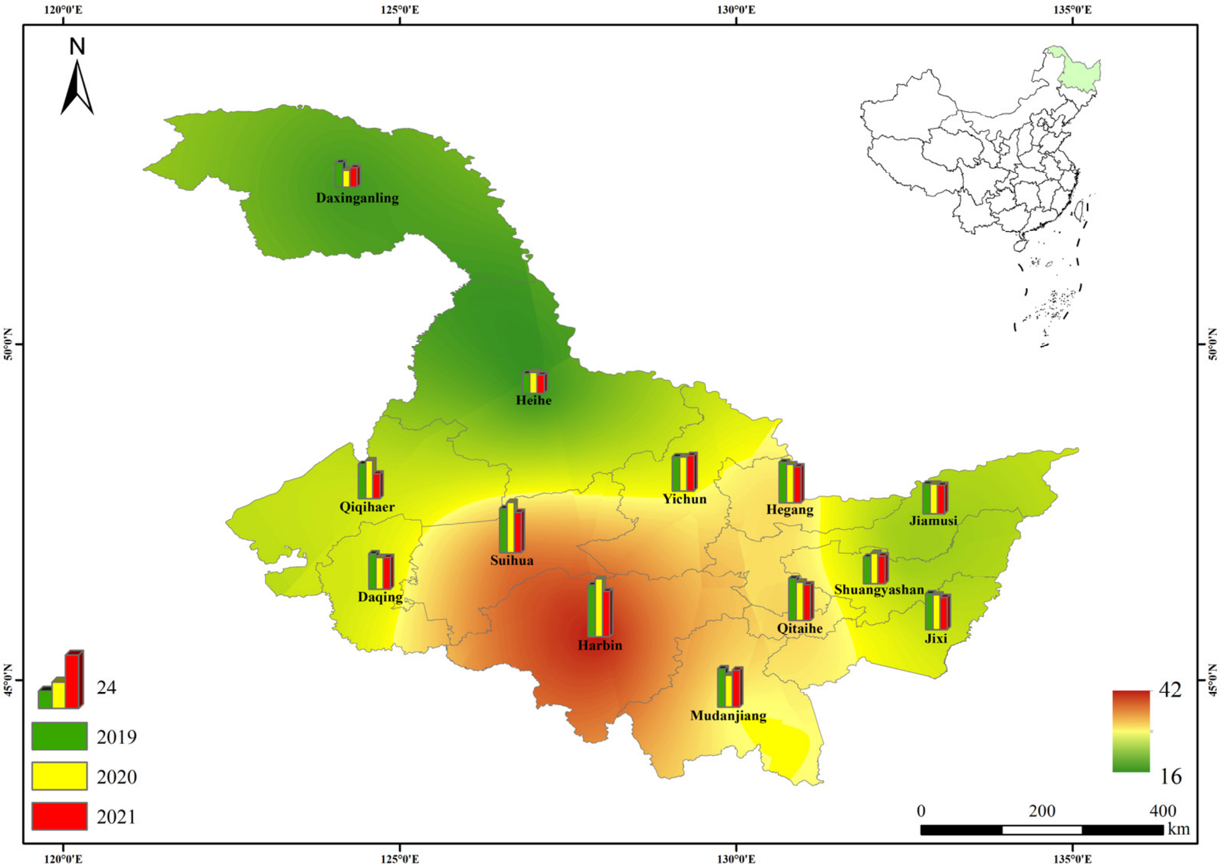

Figure 8. Changes in the annual average $PM_{2.5}$ concentrations in 13 cities in the province, 2019–2021: the background color of the map is the difference between the average values of the three years.

Urbanization progress is notably more rapid in the southern region compared with the northern region. The southern region grapples with high population density and pronounced traffic pollution issues, especially in the capital city of Harbin, which witnesses a substantial number of motor vehicles and proportionately higher exhaust emissions. Qiqihar serves as a key petrochemical base, and Daqing plays a significant role in oil production. Consequently, these industrial activities inevitably yield a certain concentration of pollutants that affect air quality. In contrast, the northwestern and northeastern regions experience lower O_3 and $PM_{2.5}$ concentrations due to flatter topography, lower average altitude, low population density, and reduced industrial pollution. Additionally, the colder climate and lower summer temperatures in the northwest hinder favorable conditions for O_3 generation, leading to the lowest O_3 concentrations.

Geographically, considering O_3's regional behavior, enhancing the collaborative prevention and control mechanism for O_3 pollution across provincial cities is crucial. Furthermore, refining the response strategy for heavily polluted $PM_{2.5}$ weather conditions in key areas is essential to comprehensively enhance air quality.

3.3. O_3 and $PM_{2.5}$ Correlation Analysis

3.3.1. Year-by-Year Correlation Analysis

As observed in Figure 9, while the overall correlation between the annual mean values of O_3 and $PM_{2.5}$ from 2019 to 2021 is modest: they all demonstrate a positive correlation and display an increasing trend year by year. Specifically, the correlation coefficients are 0.5757, 0.6072, and 0.6756 in 2019, 2020, and 2021, respectively. It is particularly noteworthy that from 2020 to 2021, the correlation coefficient increased by nearly 0.07, which is twice the increase from 2019 to 2020, indicating a progressively closer and tighter correlation between O_3 and $PM_{2.5}$.

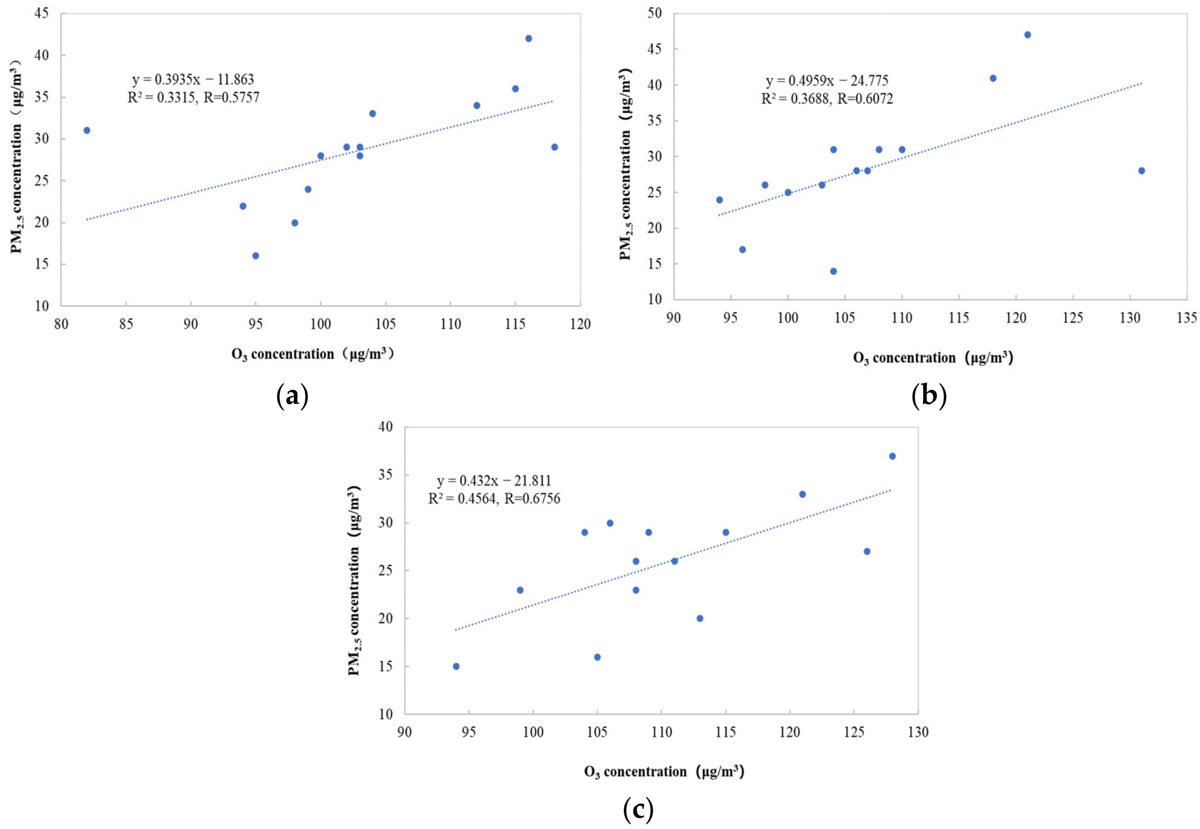

Figure 9. O_3 and $PM_{2.5}$ correlation analysis for 2019 (**a**), 2020 (**b**) and 2021 (**c**).

3.3.2. Month-by-Month Correlation Analysis

Figure 10 illustrates that the correlation between O_3 and $PM_{2.5}$ varies significantly among months, with the highest correlations occurring in the summer, followed by the spring, autumn, and winter. The average correlation coefficient for all 12 months is 0.485, with the peak correlation coefficient of 0.8814 observed in June. Notably, May also demonstrates a strong correlation coefficient of 0.7444 due to its high ozone concentration, far exceeding the average level. Conversely, January, November, and December show a negative correlation between O_3 and $PM_{2.5}$. Overall, a positive and strong correlation is evident between O_3 and $PM_{2.5}$ in months characterized by high ozone concentration and low $PM_{2.5}$ concentration, while a negative correlation is prevalent in months with low ozone concentration and high $PM_{2.5}$ concentration. Consistent with the yearly analyses, the annual mean ozone values increase annually, $PM_{2.5}$ concentrations decrease yearly, and O_3 and $PM_{2.5}$ correlations intensify yearly.

3.3.3. Correlation Analysis of Different air Quality Categories

Distinctly visible from Figure 11 is the low correlation between the different O_3 and $PM_{2.5}$ air quality categories, particularly evident in situations of good, light pollution, and moderate pollution. Presently, the primary pollutant influencing ambient air quality in Heilongjiang Province is $PM_{2.5}$, accounting for 79.0% of days exceeding limits, while O_3 contributes to 16.7% of days exceeding limits, which is a notably lower proportion compared with $PM_{2.5}$. Upon analyzing monthly correlations, it becomes apparent that while high $PM_{2.5}$ concentration months exhibit low or even negative correlations between O_3 and $PM_{2.5}$, heavily polluted and severely polluted cases present a positive correlation between the two. This emphasizes that under certain levels of $PM_{2.5}$ concentration, O_3 generation can be promoted, likely due to common pollution sources giving rise to both $PM_{2.5}$ and ozone precursor emissions, thus leading to increased O_3 concentration.

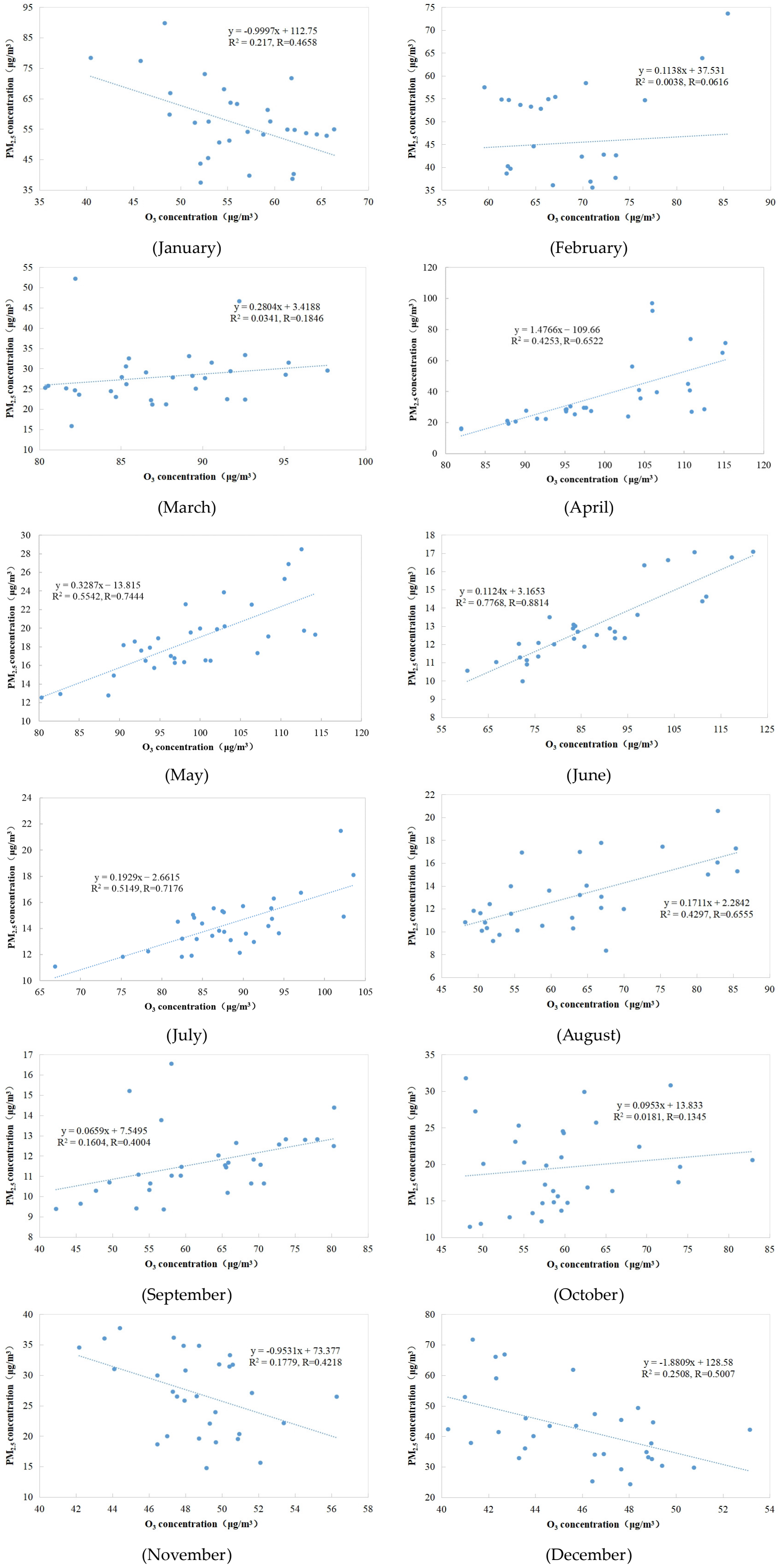

Figure 10. Correlation analysis between O_3 and $PM_{2.5}$, January–December 2019–2021.

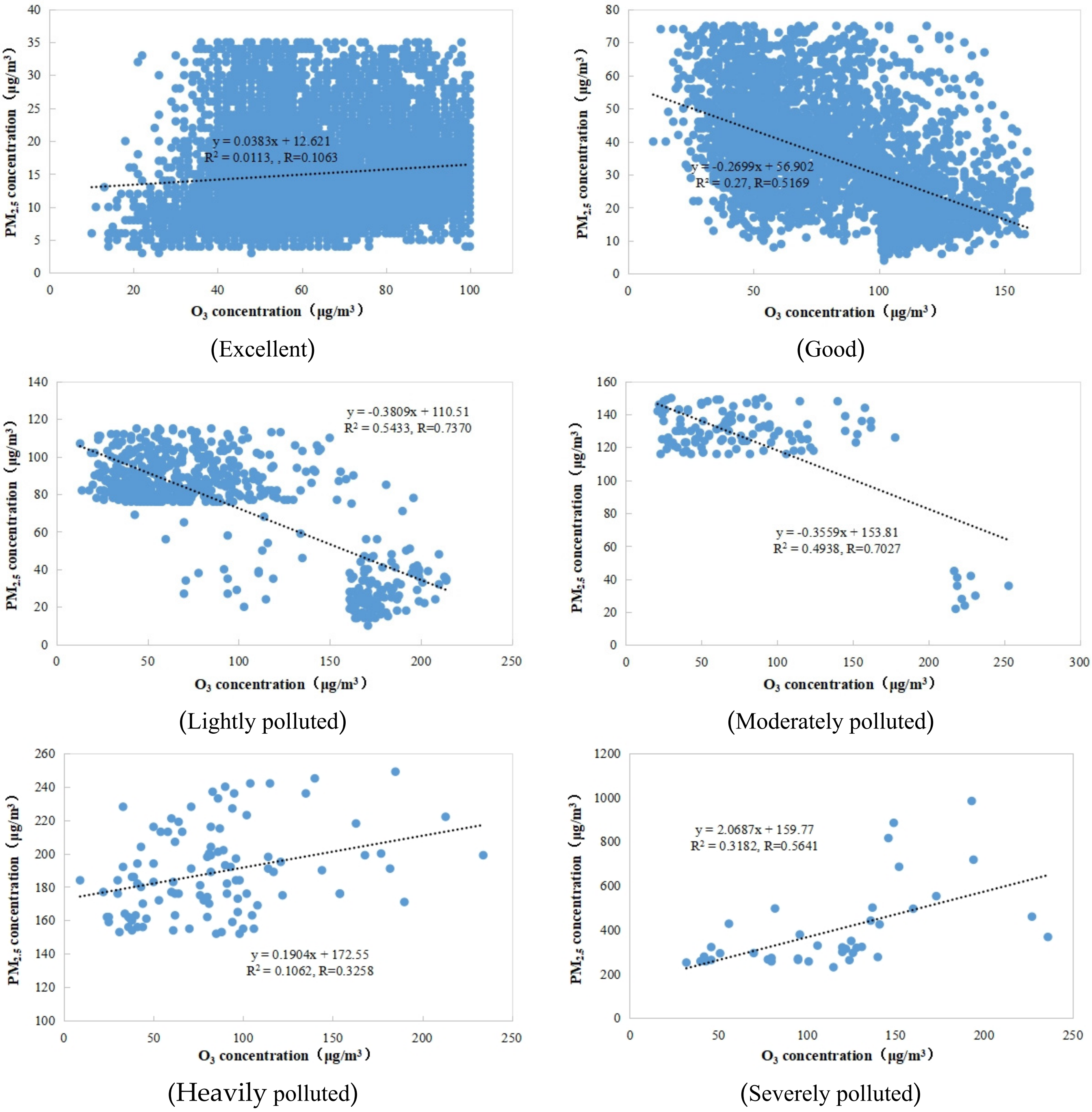

Figure 11. Correlation analysis between O_3 and $PM_{2.5}$ for different air quality categories.

4. Conclusions

In this study, we reviewed and analyzed the spatiotemporal characteristics of O_3 and $PM_{2.5}$ concentrations in Heilongjiang Province and found that the spatial and temporal variations in O_3 and $PM_{2.5}$ in Heilongjiang Province exhibit distinct characteristics. From a time perspective, there is a significant difference in the concentration changes in O_3 and $PM_{2.5}$, especially for the opposite trend in monthly changes. From a spatial perspective, the results reveal that O_3 and $PM_{2.5}$, both atmospheric pollutants, exhibit varying regional transport behaviors, generation conditions, and pollution sources. O_3 primarily forms through photochemical reactions involving VOCs and NOx under intense sunlight and high temperatures. It possesses substantial potential for long-distance transport. In contrast, $PM_{2.5}$ arises predominantly from direct emissions via combustion activities, road dust, industrial activities, and other sources or via secondary formation. Its transmission range is comparably limited.

The correlation between O_3 and $PM_{2.5}$ is higher during high ozone concentration periods, and during the air quality pollution period, it significantly surpasses the correlation during the non-pollution period, particularly during episodes of heavy and severe pollution. Additionally, this correlation progressively increases year by year. On one hand, the presence of pollutants like nitrogen oxides (NOx) influences O_3 generation, accelerating the accumulation of $PM_{2.5}$ in polluted environments. On the other hand, organic and inorganic substances within $PM_{2.5}$ serve as precursors for O_3, contributing to its generation. Consequently, the intricate relationship between O_3 and $PM_{2.5}$ necessitates acknowledgment, emphasizing the requirement for effective pollution control strategies that account for their interactions, characteristics, and influencing factors.

Source-wise, expediting source analysis for O_3 and $PM_{2.5}$ is recommended. Researching the mechanisms and coordinating control countermeasures for their formation should be pursued. Undertaking projects focused on the formation mechanism of O_3 and $PM_{2.5}$, along with their coordinated control, is vital. Completing emission source inventories and expediting the establishment of such inventories for both the province and individual cities will facilitate the formulation of targeted control strategies. This data-driven approach will provide a scientific basis for informed decisions regarding the advancement of coordinated control and joint prevention of O_3 and $PM_{2.5}$, fostering inter-regional coordination and protection of public health and living environments.

Supplementary Materials: The following supporting information can be downloaded at: https://www.mdpi.com/article/10.3390/atmos14101526/s1, Figure S1. Trends in monthly mean concentrations of O_3 in 13 cities in Heilongjiang Province in 2019 (a), 2020 (b) and 2021 (c); Figure S2. Trends in monthly mean concentrations of $PM_{2.5}$ in 13 cities in Heilongjiang Province in 2019 (a), 2020 (b) and 2021 (c).

Author Contributions: Conceptualization, P.W. and C.F.; data curation, L.X. and P.W.; formal analysis, P.W. and C.F.; investigation, R.Z.; methodology, L.L. and Y.X.; resources, L.L.; software, R.Z.; visualization, Y.X.; writing—original draft, P.W. and C.F.; writing—review and editing, L.X. and Y.X. All authors have read and agreed to the published version of this manuscript.

Funding: This research did not receive a specific grant from any funding agencies in the public, commercial, or non-for-profit sectors.

Institutional Review Board Statement: Not applicable.

Informed Consent Statement: Not applicable.

Data Availability Statement: The data presented in this study are available on request from the corresponding author.

Conflicts of Interest: The authors declare no conflict of interest.

References

1. Duan, W.; Wang, X.; Cheng, S.; Wang, R. Regional collaboration to simultaneously mitigate $PM_{2.5}$ and O_3 pollution in Beijing-Tianjin-Hebei and the surrounding area: Multi-model synthesis from multiple data sources. *Sci. Total Environ.* **2022**, *820*, 153309. [CrossRef] [PubMed]
2. Gong, S.; Liu, Y.; He, J.; Zhang, L.; Lu, S.; Zhang, X. Multi-scale analysis of the impacts of meteorology and emissions on $PM_{2.5}$ and O_3 trends at various regions in China from 2013 to 2020 1: Synoptic circulation patterns and pollution. *Sci. Total Environ.* **2022**, *815*, 152770. [CrossRef] [PubMed]
3. Duan, W.; Wang, X.; Cheng, S.; Wang, R. Regional division and influencing mechanisms for the collaborative control of $PM_{2.5}$ and O_3 in China: A joint application of multiple mathematic models and data mining technologies. *J. Clean. Prod.* **2022**, *337*, 130607. [CrossRef]
4. Qiao, L.; Chen, Z.; Takada, C.; Chiba, H.; Inoue, K.; Hui, S.; Ye, S. Quantitative evaluation on the degradation process of the pulmonary surfactant monolayer when exposed to low-level ozone of ambient environment. *Anal. Chem.* **2022**, *94*, 8651–8658. [CrossRef] [PubMed]
5. Liang, S.; Sha, Y.; Yang, C.; Lai, H.; Sun, C.; Zhao, W.; Zhang, A.; Qi, Q.; Xie, Y. Ozone-Induced Lung and Bronchial Injury: A Mouse Model Study. *Atmosphere* **2022**, *13*, 1562. [CrossRef]

6. Yu, R.; Lin, Y.; Zou, J.; Dan, Y.; Cheng, C. Review on atmospheric ozone pollution in China: Formation, spatiotemporal distribution, precursors and affecting factors. *Atmosphere* **2021**, *12*, 1675. [CrossRef]
7. Hodgson, J.R.; Chapman, L.; Pope, F.D. The Diamond League athletic series: Does the air quality sparkle? *Int. J. Biometeorol.* **2021**, *65*, 1427–1442. [CrossRef]
8. Pleijel, H.; Danielsson, H.; Broberg, M.C. Benefits of the Phytotoxic Ozone Dose (POD) index in dose-response functions for wheat yield loss. *Atmos. Environ.* **2022**, *268*, 118797. [CrossRef]
9. Sharps, K.; Hayes, F.; Harmens, H.; Mills, G. Ozone-induced effects on leaves in African crop species. *Environ. Pollut.* **2021**, *268*, 115789. [CrossRef]
10. Lin, H.; Chen, M.; Gao, Y.; Wang, Z.; Jin, F. Tussilagone protects acute lung injury from $PM_{2.5}$ via alleviating Hif-1α/NF-κB-mediated inflammatory response. *Environ. Toxicol.* **2022**, *37*, 1198–1210. [CrossRef]
11. Sun, W.; Huo, J.; Li, R.; Wang, D.; Yao, L.; Fu, Q.; Feng, J. Effects of energy structure differences on chemical compositions and respiratory healthof $PM_{2.5}$ during late autumn and winter in China. *Sci. Total Environ.* **2022**, *824*, 153850. [CrossRef] [PubMed]
12. Kim, J.; Lee, D.G.; Wang, L.; Kang, H.; Hwang, M. Acute Moderate-Intensity Aerobic Exercise under High $PM_{2.5}$ Levels Does Not Influence the Pulmonary Function and Lung Diffusion Capacity in Healthy Young Men. *Appl. Sci.* **2022**, *12*, 10080. [CrossRef]
13. Hopke, P.K.; Hidy, G. Changing emissions results in changed $PM_{2.5}$ composition and health impacts. *Atmosphere* **2022**, *13*, 193. [CrossRef]
14. Wong, Y.K.; Huang, X.H.; Cheng, Y.Y.; Yu, J.Z. Estimating primary vehicular emission contributions to $PM_{2.5}$ using the chemical mass balance model: Accounting for gas-particle partitioning of organic aerosols and oxidation degradation of hopanes. *Environ. Pollut.* **2021**, *291*, 118131. [CrossRef] [PubMed]
15. Guo, X.; Wang, Y.; Mei, S.; Shi, C.; Liu, Y.; Pan, L.; Li, K.; Zhang, B.; Wang, J.; Zhong, Z. Monitoring and modelling of $PM_{2.5}$ concentration at subway station construction based on IoT and LSTM algorithm optimization. *J. Clean. Prod.* **2022**, *360*, 132179. [CrossRef]
16. Tian, Y.; Liu, X.; Huo, R.; Shi, Z.; Sun, Y.; Feng, Y.; Harrison, R.M. Organic compound source profiles of $PM_{2.5}$ from traffic emissions, coal combustion, industrial processes and dust. *Chemosphere* **2021**, *278*, 130429. [CrossRef]
17. Yang, C.; Hong, Z.; Chen, J.; Xu, L.; Zhuang, M.; Huang, Z. Characteristics of secondary organic aerosols tracers in $PM_{2.5}$ in three central cities of the Yangtze river delta, China. *Chemosphere* **2022**, *293*, 133637. [CrossRef]
18. Liu, Y.; Yang, Z.; Liu, Q.; Qi, X.; Qu, J.; Zhang, S.; Wang, X.; Jia, K.; Zhu, M. Study on chemical components and sources of $PM_{2.5}$ during heavy air pollution periods at a suburban site in Beijing of China. *Atmos. Pollut. Res.* **2021**, *12*, 188–199. [CrossRef]
19. Cheng, M.; Tang, G.; Lv, B.; Li, X.; Wu, X.; Wang, Y.; Wang, Y. Source apportionment of $PM_{2.5}$ and visibility in Jinan, China. *J. Environ. Sci.* **2021**, *102*, 207–215. [CrossRef]
20. Zhang, T.; Shen, Z.X.; Su, H.; Liu, S.X.; Zhou, J.M.; Zhao, Z.Z.; Wang, Q.Y.; Prévôt, A.; Cao, J.J. Effects of Aerosol Water Content on the formation of secondary inorganic aerosol during a Winter Heavy $PM_{2.5}$ Pollution Episode in Xi'an, China. *Atmos. Environ.* **2021**, *252*, 118304. [CrossRef]
21. Sharma, A.; Valdes, A.C.F.; Lee, Y. Impact of Wildfires on Meteorology and Air Quality ($PM_{2.5}$ and O_3) over Western United States during September 2017. *Atmosphere* **2022**, *13*, 262. [CrossRef]
22. Zhang, Q.; Pan, Y.; He, Y.; Walters, W.W.; Ni, Q.; Liu, X.; Xu, G.; Shao, J.; Jiang, C. Substantial nitrogen oxides emission reduction from China due to COVID-19 and its impact on surface ozone and aerosol pollution. *Sci. Total Environ.* **2021**, *753*, 142238. [CrossRef] [PubMed]
23. Liu, Z.; Qi, Z.; Ni, X.; Dong, M.; Ma, M.; Xue, W.; Zhang, Q.; Wang, J. How to apply O_3 and $PM_{2.5}$ collaborative control to practical management in China: A study based on meta-analysis and machine learning. *Sci. Total Environ.* **2021**, *772*, 145392. [CrossRef] [PubMed]
24. Ke, Y.; Liu, R.; Chen, X.; Feng, Y.; Gao, P.; Huang, H.; Fan, L.; Ye, D. Volatile organic compounds concentration profiles and control strategy in container manufacturing industry: Case studies in China. *J. Environ. Sci.* **2021**, *104*, 296–306. [CrossRef]
25. Li, J.; Han, Z.; Zhang, R. Influence of aerosol hygroscopic growth parameterization on aerosol optical depth and direct radiative forcing over East Asia. *Atmos. Res.* **2014**, *140–141*, 14–27. [CrossRef]
26. Jia, M.; Zhao, T.; Cheng, X.; Gong, S.; Zhang, X.; Tang, L.; Liu, D.; Wu, X.; Wang, L.; Chen, Y. Inverse relations of $PM_{2.5}$ and O_3 in air compound pollution between cold and hot seasons over an urban area of east China. *Atmosphere* **2017**, *8*, 59. [CrossRef]
27. Li, X.; Bei, N.; Wu, J.; Wang, R.; Liu, S.; Liu, L.; Jiang, Q.; Tie, X.; Molina, L.T.; Li, G. Heterogeneous HONO formation deteriorates the wintertime particulate pollution in the Guanzhong Basin, China. *Environ. Pollut.* **2022**, *303*, 119157. [CrossRef]
28. Shao, M.; Wang, W.; Yuan, B.; Parrish, D.D.; Li, X.; Lu, K.; Wu, L.; Wang, X.; Mo, Z.; Yang, S. Quantifying the role of $PM_{2.5}$ dropping in variations of ground-level ozone: Inter-comparison between Beijing and Los Angeles. *Sci. Total Environ.* **2021**, *788*, 147712. [CrossRef]
29. Wang, W.; Parrish, D.D.; Li, X.; Shao, M.; Liu, Y.; Mo, Z.; Lu, S.; Hu, M.; Fang, X.; Wu, Y. Exploring the drivers of the increased ozone production in Beijing in summertime during 2005–2016. *Atmos. Chem. Phys.* **2020**, *20*, 15617–15633. [CrossRef]
30. Wang, P.; Qiao, X.; Zhang, H. Modeling $PM_{2.5}$ and O_3 with aerosol feedbacks using WRF/Chem over the Sichuan Basin, southwestern China. *Chemosphere* **2020**, *254*, 126735. [CrossRef]
31. Tie, X.; Long, X.; Li, G.; Zhao, S.; Cao, J.; Xu, J. Ozone enhancement due to the photodissociation of nitrous acid in eastern China. *Atmos. Chem. Phys.* **2019**, *19*, 11267–11278. [CrossRef]

32. Lu, C.; Mao, J.; Wang, L.; Guan, Z.; Zhao, G.; Li, M. An unusual high ozone event over the North and Northeast China during the record-breaking summer in 2018. *J. Environ. Sci.* **2021**, *104*, 264–276. [CrossRef]
33. Liu, X.; Guo, H.; Zeng, L.; Lyu, X.; Wang, Y.; Zeren, Y.; Yang, J.; Zhang, L.; Zhao, S.; Li, J.; et al. Photochemical ozone pollution in five Chinese megacities in summer 2018. *Sci. Total Environ.* **2021**, *801*, 149603. [CrossRef] [PubMed]
34. Jakovljević, T.; Lovreškov, L.; Jelić, G.; Anav, A.; Popa, I.; Fornasier, M.F.; Proietti, C.; Limić, I.; Butorac, L.; Vitale, M.; et al. Impact of ground-level ozone on Mediterranean forest ecosystems health. *Sci. Total Environ.* **2021**, *783*, 147063. [CrossRef] [PubMed]
35. Tadic, I.; Nussbaumer, C.M.; Bohn, B.; Harder, H.; Marno, D.; Martinez, M.; Obersteiner, F.; Parchatka, U.; Pozzer, A.; Rohloff, R. Central role of nitric oxide in ozone production in the upper tropical troposphere over the Atlantic Ocean and western Africa. *Atmos. Chem. Phys.* **2021**, *21*, 8195–8211. [CrossRef]
36. Feng, X.; Feng, Y.; Chen, Y.; Cai, J.; Li, Q.; Chen, J. Source apportionment of $PM_{2.5}$ during haze episodes in Shanghai by the PMF model with PAHs. *J. Clean. Prod.* **2022**, *330*, 129850. [CrossRef]
37. He, C.; Hong, S.; Mu, H.; Tu, P.; Yang, L.; Ke, B.; Huang, J. Characteristics and Meteorological Factors of Severe Haze Pollution in China. *Adv. Meteorol.* **2021**, *2021*, 6680564. [CrossRef]
38. Chen, B.; Liu, M.; Ye, W.; Zhang, B. Assessing the impact of green nudges on ozone concentration: Evidence from China's night refueling policy. *J. Environ. Manag.* **2022**, *312*, 114899. [CrossRef]
39. Yang, X.; Wu, K.; Lu, Y.; Wang, S.; Qiao, Y.; Zhang, X.; Wang, Y.; Wang, H.; Liu, Z.; Liu, Y.; et al. Origin of regional springtime ozone episodes in the Sichuan Basin, China: Role of synoptic forcing and regional transport. *Environ. Pollut.* **2021**, *278*, 116845. [CrossRef]
40. Zhang, G.; Jing, S.; Xu, W.; Gao, Y.; Yan, C.; Liang, L.; Huang, C.; Wang, H. Simultaneous observation of atmospheric peroxyacetyl nitrate and ozone in the megacity of Shanghai, China: Regional transport and thermal decomposition. *Environ. Pollut.* **2021**, *274*, 116570. [CrossRef]
41. Wang, H.; Ding, K.; Huang, X.; Wang, W.; Ding, A. Insight into ozone profile climatology over northeast China from aircraft measurement and numerical simulation. *Sci. Total Environ.* **2021**, *785*, 147308. [CrossRef] [PubMed]
42. Gong, K.; Li, L.; Li, J.; Qin, M.; Wang, X.; Ying, Q.; Liao, H.; Guo, S.; Hu, M.; Zhang, Y.; et al. Quantifying the impacts of inter-city transport on air quality in the Yangtze River Delta urban agglomeration, China: Implications for regional cooperative controls of $PM_{2.5}$ and O_3. *Sci. Total Environ.* **2021**, *779*, 146619. [CrossRef] [PubMed]
43. Yan, Y.; Cai, X.; Miao, Y.; Yu, M. Synoptic condition and boundary layer structure regulate $PM_{2.5}$ pollution in the Huaihe River Basin, China. *Atmos. Res.* **2022**, *269*, 106041. [CrossRef]
44. Guan, P.; Wang, X.; Cheng, S.; Zhang, H. Temporal and spatial characteristics of $PM_{2.5}$ transport fluxes of typical inland and coastal cities in China. *J. Environ. Sci.* **2021**, *103*, 229–245. [CrossRef] [PubMed]
45. Shi, J.; Feng, Y.; Ren, L.; Lu, X.; Zhong, Y.; Han, X.; Ning, P. Mass concentration, chemical composition, and source characteristics of $PM_{2.5}$ in a plateau slope city in southwest China. *Atmosphere* **2021**, *12*, 611. [CrossRef]